EUROPEAN FUSION DEVELOPMENT AGREEMENT

EFDA–JET–CP(04)07-36

T. Tala, C. Bourdelle, F. Imbeaux, D. Moreau, V. Parail, G. Corrigan, F. Crisanti, X. Garbet, D. Heading, E. Joffrin, L. Laborde, X. Litaudon, P. Mantica, D. Mazon, A. Salmi, P. Strand, J. Weiland, ITPA Topical Group on Transport Physics and the ITB Database Working Group and JET EFDA Contributors

Progress in Transport Modelling of Internal Transport Barrier Plasmas in JET

Progress in Transport Modelling of Internal Transport Barrier Plasmas in JET

T. Tala[1], C. Bourdelle[2], F. Imbeaux[2], D. Moreau[2], V. Parail[3], G. Corrigan[3], F. Crisanti[3], X. Garbet[2], D. Heading[3], E. Joffrin[2], L. Laborde[2], X. Litaudon[2], P. Mantica[5], D. Mazon[2], A. Salmi[6], P. Strand[7], J. Weiland[7], ITPA Topical Group on Transport Physics and the ITB Database Working Group[8] and JET EFDA Contributors*

[1]Association EURATOM-Tekes, VTT Processes, P.O. Box 1608, FIN-02044 VTT, Finland
[2]Association EURATOM-CEA, CEA/DSM/DRFC Cadarache, St Paul-Lez-Durance, France
[3]EURATOM/UKAEA Fusion Association, Culham Science Centre, Oxon. OX14 3DB, UK
[4]Associazione EURATOM-ENEA sulla Fusione, Via Enrico Fermi 27, 00044 Frascati, Italy
[5]Istituto di Fisica del Plasma CNR-EURATOM, via Cozzi 53, 20125 Milano, Italy
[6]Association EURATOM-Tekes, Helsinki University of Technology, FIN-02015, TKK, Finland
[7]Association EURATOM-VR, Chalmers University of Technology, Göteborg, Sweden
[8]See Gohil Pet al., Nuclear Fusion, 43, 708 (2003)
** See annex of J. Pamela et al, "Overview of JET Results ", (Proc.20 [th] IAEA Fusion Energy Conference, Vilamoura, Portugal (2004).*

Preprint of Paper to be submitted for publication in Proceedings of the 20th IAEA Conference, (Vilamoura, Portugal 1-6 November 2004)

ABSTRACT.
This paper will report on the recent progress in transport modelling of Internal Transport Barrier (ITB) plasmas. Two separate issues will be covered, fully predictive transport modelling of ITBs in the multi-tokamak database, including micro-stability analyses of ITBs, and predictive closed-loop (i.e. real-time control) transport simulations of the *q*-profile and ITBs. For the first time, the predictive capabilities of the mixed Bohm/GyroBohm and Weiland transport models are investigated with discharges from the ITPA ITB database by fully predictive transport simulations. The predictive transport simulations with the Bohm/GyroBohm model agree very well with experimental results from JET and JT-60U. In order to achieve a good agreement in DIII-D, the α-stabilisation had to be included into the model, showing the significant role played by the α-stabilisation in governing the physics of the ITBs. The significant role of the α-stabilisation is also emphasised by the gyro-kinetic analysis. The Weiland transport model shows only limited agreement between the model predictions and experimental results with respect to the formation and location of the ITB. The fully predictive closed-loop simulations with real-time control of the *q*-profile and ITB show that it is possible to reach various set-point profiles for *q* and ITB and control them for longer than a current diffusion time in JET using the same real-time control technique as in the experiments.

1. PREDICTIVE TRANSPORT MODELLING AND MICRO-STABILITY OF ITBS

The question of the ITB formation and dynamics is assessed with fully predictive transport modelling and micro-stability analyses. In the predictive transport simulations, five transport equations (electron and ion heat, *q*, density and toroidal momentum) are solved, the latter two being essential for the most realistic and consistent understanding of the ITB behaviour. One high performance JET discharge with a low positive or zero magnetic shear (*s*) and another one with negative *s* are simulated with two different transport models, Bohm/GyroBohm [1] and Weiland [2], using the JETTO transport code. In order to see whether the transport models perform similarly in other tokamaks, two discharges with similarly different magnetic shear from JT-60U and DIII-D are simulated and compared. Having discharges from three different tokamaks enables us to recognise common and non-common features of ITB formation and dynamics between different tokamaks. More importantly, it is possible to perform a cross-tokamak ITB/transport model validation — a critical step necessary to improve the predictability of the ITB plasma scenario in the next step devices. All the necessary input data for the three pairs of discharges from JET, JT-60U and DIII-D are taken from the multi-tokamak ITPA ITB database [3,4,5] located presently in Culham, UK. The input data include the geometry, the power deposition profiles, the external current density profiles, torque, Z_{eff} as well as the initial and boundary conditions for the transport equations to be solved. The main plasma parameters of the discharges are shown in Table I. ITB formation in the semi-empirical Bohm/GyroBohm model is based on turbulence suppression by the combined effects of *s* and $\omega_{E\times B}$ flow shear [1]. The standard Bohm/GyroBohm model is modified to include the α-stabilisation [6] ($\alpha = -2Rq^2\nabla P\mu_0/B^2$). The resulting ITB formation threshold condition with α included takes the following form:

$$0.5 + s - \frac{\omega_{E\times B}}{\gamma_{ITG}} - 0.6\,\alpha < 0. \quad (1)$$

Here γ_{ITG} represents a simple approximation of the linear growth rate defined as $\gamma_{ITG} = v_{th}/R$ (v_{th} is the ion thermal velocity and R the major radius). The Weiland model includes also turbulence suppression by the α-stabilisation ($\alpha = -2Rq^2\nabla P\mu_0/B^2$), that of density peaking [7] and the dilution effect [8]. To calculate the anomalous toroidal momentum diffusivity (viscosity), both the Bohm/GyroBohm and Weiland models use the assumption that $\chi_{mom} = \chi_i$.

TABLE I: THE SIMULATED DISCHARGES FROM THE ITPA ITB DATABASE.

Tokamak	Pulse No.	I_p [MA]	B_ϕ [T]	P_{in} [MW]	Reversed q
JET	46664	3.4	3.4	22	no
JET	53521	2.0	3.4	22	yes
JT-60U	34487	1.5	3.7	13	no
JT-60U	39056	1.3	3.7	8	yes
DIII-D	87031	1.6	2.1	9	no
DIII-D	95989	1.6	2.1	5	yes

The fully predictive (density n_e, electron temperature T_e, ion temperature T_i, q and toroidal rotation v_Φ predicted), time-dependent simulations for each discharge are performed for the whole time (varying from 0.4s until 9.0s) that exists in the ITB database. The time-dependent simulations are crucial because the ITB discharges are usually not in steady-state, for example with respect to the q-profile evolution as illustrated in figure 1.

Figures 2–4 illustrate the five predicted plasma profiles as well as the experimental values for the three pairs of discharges from JET, JT-60U and DIII-D in the respective order at the last time point of each simulation (except v_Φ is replaced with the neo-classical parallel velocity $v_{||}$ in JT-60U due to negligible v_Φ originating from the balanced NBI). In all the three figures, the label scheme is as follows: the solid black curves correspond to the experimental data from the ITPA ITB database, and the red dashed and blue dash-dotted curves to the simulation predictions by the mixed Bohm/GyroBohm and Weiland transport models, respectively. Also in each figure 2–4, the plots on the left-hand side present the data and simulation results for the discharge with a monotonic or flat q-profile and on the right-hand side for the discharge with a reversed q-profile in each tokamak, respectively.

With the Bohm/GyroBohm model (red dashed curves), the agreement with respect to the radial location and dynamics of the ITB between the experiments and transport simulations is good in JET (figure 2). In JT-60U (figure 3), the model performs as well as in JET, but in DIII-D the agreement is worse (figure 4). This suggests that the empirical ITB threshold condition derived from JET database (combined effect of the magnetic shear and $\omega_{E\times B}$ flow shear) is able to reproduce

the dynamics of the ITBs well in JET and in a similar size tokamak JT-60U. However, in a smaller size tokamak DIII-D, the α-stabilisation had to be taken into account to in order to obtain the same level of agreement between the modelling predictions and experiments among the three tokamaks. The role of α-stabilisation in governing the ITB dynamics is confirmed in gyro-kinetic simulations [9]. When including the α-stabilisation in the ITB threshold condition (formula (1)), the agreement improves significantly in DIII-D, as illustrated in figure 5, while only minor changes can be observed in JET and JT-60U.

The Weiland model (blue dash-dotted curves in figures 1–4) did not predict a clear ITB in any of the six simulated discharges. Because of this, in most of the simulations it tended to underestimate the central values of the predicted quantities, in particular the ion temperature. The growth rates of the unstable modes predicted by the Weiland model were 2–10 times higher than the $\omega_{E\times B}$ shearing rates. Typically a factor of larger than 10 is needed to multiply the $\omega_{E\times B}$ shearing rate in order to obtain an ITB. The growth rates of the unstable modes calculated with a gyro-kinetic flux tube code KINEZERO [10] are lower than those predicted by the Weiland model and in rough agreement with the $\omega_{E\times B}$ shearing rates at the location of the ITB. At this point we need to comment that the growth rates predicted by the Weiland model are extreme sensitive to the value and profile of Z_{eff}. Changing Z_{eff} by 20% may be enough to trigger a clear ITB and the uncertainties in Z_{eff} taken from the database can be of that order. Another related reason, in addition to the discrepancies between the $\omega_{E\times B}$ shearing and growth rates, for the Weiland model not to give satisfactory predictions for ITBs is that the effect of the magnetic shear on transport seems to be too weak. In fact, the effect of the magnetic shear on transport in the Weiland model is much weaker than experimentally observed or that in the Bohm/GyroBohm model. However, there is a new version of the Weiland model to be released soon, which has varying correlation lengths and a much stronger dependence on magnetic shear and q [11]. The preliminary results with the modified model are encouraging.

The key question to be raised is how reliably we can predict the behaviour of the ITB plasmas in future devices, for example in ITER. The semi-empirical Bohm/GyroBohm model with its ITB formation threshold condition was derived empirically from JET ITB plasmas. Although it works very well in JET and in a similar size tokamak JT-60U, and also in a smaller size tokamak DIII-D when including the ±-stabilisation, it does not prove that the same modelling capability and accuracy can be extrapolated to much larger size tokamaks. On the other hand, the predictions with the first-principle transport models, like the Weiland model, are not in a satisfactory agreement even with the experimental results from the present tokamaks. In addition, an ITB/transport model must be able to predict the time evolution of ITB plasmas under a varying q-profile and other plasma profiles and parameters, not just be able to predict a stationary ITB at one time slice. This is a real problem for the development of advanced tokamak scenarios for ITER, where a proper alignment between the ITB and non-inductive current is critical for steady-state operation. Whether this alignment can be reached or not, depends strongly on the coupling mechanisms between the pressure and current profiles, among them all those underlying the ITB physics. Therefore, future efforts must be further

directed towards clarifying the role of different stabilisation mechanisms ($\omega_{E\times B}$ shearing rate, magnetic shear, α-stabilisation, role of rational q surfaces, ...), as well as the magnitude of turbulence suppression within the ITB. And finally that physics should be implemented into a reliable first-principle transport model, in view of developing advanced tokamak scenarios for steady-state operation in ITER.

2. FULLY PREDICTIVE CLOSED-LOOP SIMULATIONS WITH RTC OF THE *Q*-PROFILE AND ITB

For the first time fully predictive transport simulations with a nonlinear plasma model (Bohm/GyroBohm transport model) have been used in closed-loop simulations to control the q-profile and the strength and location of the ITB. Five transport equations (T_e, T_i, q, n_e, v_Φ) are solved and the power levels of LHCD, NBI and ICRH are calculated in a feedback loop and depend on the difference between the set-point (target) and the simulated profiles of q and ρ_t^* (the ratio between the Larmor radius and the electron temperature gradient length). A description of the profile control algorithm used in these simulations can be found in Ref. [12]. The power deposition and driven current density profiles of the three actuators are calculated as follows: FRTC [13] for LHCD, PENCIL [14] for NBI and PION [15] for ICRH. LHCD and NBI, which are sensitive to variations in plasma profiles, are calculated self-consistently inside JETTO whereas the ICRH power deposition profile is prescribed by the PION calculation. The power levels of the three actuators in closed-loop simulations, i.e. when applying the RTC technique, are fully determined from the difference between the set-point (target) and simulated values of q and ρ_t^* multiplied by the feedback control matrix.

The feedback control matrix has been calculated from the open-loop JETTO transport simulations with power step-ups/downs using the same Bohm/GyroBohm transport model as later in closed-loop simulations. The feedback control algorithms in JETTO are modular and independent of the choice of the transport model. The procedure of calculating the feedback control matrix from the open-loop simulations using the steady-state response of q and ρ_t^* to the power step-ups is identical to the experimental one, including the projection of q and ρ_t^* on the set of basis functions by using the Galerkin scheme [16]. The status of the experimental results with the real-time control of q and ρ_t^* in JET has been presented in Ref. [17] and will also be presented in this conference [18].

Two closed-loop simulations with different set-point profiles of q and ρ_t^* are compared with a reference open-loop simulation with constant power levels in figures 5 and 6. The set-point profiles in the two closed-loop simulations are given as follows: first simulation (red curves) has monotonic$q$ and no ITB (small ρ_t^*) and the second simulation (blue curves) has deeply reversed$q$ and strong ITB (large ρ^*). The set-point profiles are illustrated in figures 7 and 8 by the dashed lines using the same colour scheme. The magnetic field, plasma current, geometry, Z_{eff}, the power levels of LHCD, ICRH and NBI until the control starts at t=45.5s as well as the initial and boundary conditions are taken from JET pulse no. 62527. This pulse has been one of the most successful RTC experiments with a simultaneous control of q and ρ_t^* on JET [13]. However, the closed-loop simulations are

extended much further in time to reach the time scale of the current diffusion time than the experiment itself that ended after t=49s.

As one can see in figures 5 and 6, the three simulations start to deviate from each other immediately after t=45.5s when the real-time control starts. The simulated and the set-point q-profiles and ρ_t^* profiles for the same three simulations with the same colours are illustrated in figures 7 and 8. The closed-loop simulation (red solid) with a monotonic q and no ITB as the set-point values (green dashed) as well as the open-loop reference simulation (black solid) is presented in figure 7. The other closed-loop simulation (blue solid) with a reversed q and strong ITB as the set-point profiles (green dashed) as well as the same reference simulation (black solid) is shown in figure 8. The regions where the control is applied to are for q $0.2<\rho<0.8$ and for ρ_t^* $0.4<\rho<0.6$ (r being the normalised radial coordinate).

The closed-loop simulations in figures 7 and 8 show that varieties of set-point q-profiles and ρ_t^* profiles are possible to achieve and control simultaneously. The time when the set-point values are reached may be of the order of current diffusion time (~10–20s), i.e. longer than that can be experimentally demonstrated. The reason for the longer time to reach the set-point profiles in the simulations than observed in the experiments is that in these simulations the initial q and ρ_t^* profiles have been further from the set-point profiles than those in the experiments. Thus, a smaller overall gain multiplying the controller has been used in simulations.

These simulations support strongly the experimental results that the real-time control of q and ρ_t^* profiles can be carried out using the present multi-input multi-output model, its singular value decomposition which then allows a distributed-parameter real-time controller to be designed. In order to circumvent the problem of handling two different time scales in the controller (ITB evolves within the confinement time whereas q-profile evolves within the resistive current diffusion time), a multiple time scale controller is being designed and will be tested in JETTO transport simulations in future.

CONCLUSIONS

This paper reported on the recent progress in transport modelling of ITB plasmas in JET. Two separate issues were presented, fully predictive transport modelling of ITBs in the multi-tokamak database and predictive closed-loop transport simulations of the q-profile and ITBs. The predictive transport simulations with the Bohm/GyroBohm model agreed very well with experimental results from JET and JT-60U. In order to reproduce ITBs within the same good accuracy also in DIII-D, the $\pm$-stabilisation had to be included into the model. Having modelled tokamaks with different sizes demonstrated the significant role played by the $\pm$-stabilisation in governing the physics of the ITBs. The Weiland transport model showed only limited agreement between the model predictions and experimental results with respect to the formation and location of the ITB. A new version of the model with stronger dependencies on magnetic shear and q yields encouraging results. The fully predictive closed-loop simulations with real-time control of the q-profile and ITB demonstrated

that it is possible to reach various set-point profiles for *q* and ITB and control them for longer than a resistive current diffusion time in JET using the same real-time control technique as in the experiments.

REFERENCES:

[1]. T. Tala et al., *Plasma Phys. Control. Fusion*, **43**, 507 (2001).

[2]. J. Weiland, ''Collective Modes in Inhomogeneous Plasma'', Institute of Physics Publishing, Bristol, (2000).

[3]. T. Fukuda et al., 28th EPS Conference, Madeira, 2001, ECA Vol. **25A**, P-5.115.

[4]. P. Gohil et al., *Nucl. Fusion*, **43**, 708 (2003).

[5]. X. Litaudon et al., *Plasma Phys. Control. Fusion*, **46**, A19 (2004).

[6]. M.A. Beer et al., *Phys. Plasmas*, **4**, 1972 (1997).

[7]. G.M. Staebler et al., *Plasma Phys. Control. Fusion*, **40**, 569 (1998).

[8]. J. Weiland, 28th EPS Conference, Madeira, 2001, ECA Vol **25A**, P2.039.

[9]. C. Bourdelle et al.,"Impact of α on the microstability of internal transport barriers", submitted to *Nucl. Fusion* (2004).

[10]. C. Bourdelle et al., *Nucl. Fusion*, **42**, 892 (2002).

[11]. J. Weiland and I. Holod, "Drift wave transport scalings introduced by varying correlation length", accepted for publication in Phys. Plasmas (2004).

[12]. D. Moreau et al., *Nucl. Fusion*, **43**, 870 (2003).

[13]. A.R. Esterkin and A.D. Piliya., *Nucl. Fusion*, **36**, 1231 (1996).

[14]. C.D. Challis et al., *Nucl. Fusion*, **29**, 563 (1989).

[15]. L.-G. Eriksson, T. Hellsten, U. Willen, *Nucl. Fusion*, **33**, 1037 (1993).

[16] L. Laborde et al., "A model-based technique for real-time control of current and pressure profiles in the JET tokamak", submitted to *Plasma Phys. Control. Fusion* (2004).

[17] D. Mazon et al., 31st EPS Conference, London, 2004, ECA Vol **28G**, P5.168.

[18] D. Moreau et al., "Development of Integrated Real-Time Control of Internal Transport Barriers in Advanced Operation Scenarios on JET", this conference.

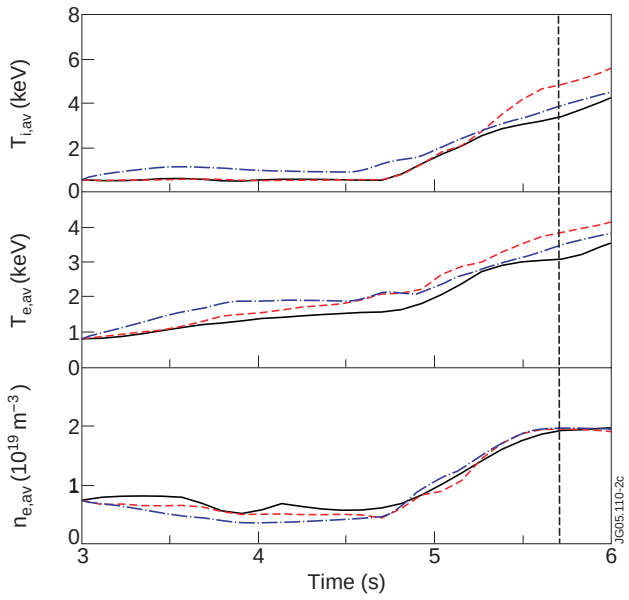

Figure 1: Time evolution of the averaged T_i, T_e and n_e for JET Pulse No: 46664.The black solid curve represents the experimental data and the red dashed and blue dash-dotted curves the simulation predictions by the Bohm/ GyroBohm and Weiland models, respectively. The green dashed line indicates the time for the onset of the ITB.

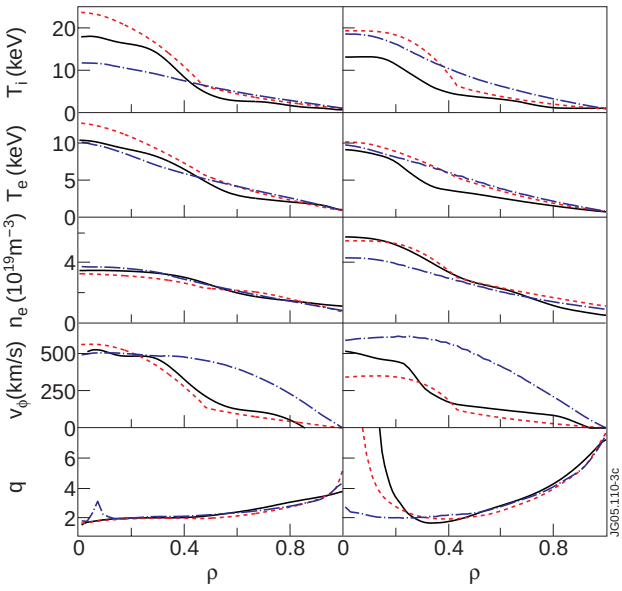

Figure 2: Comparison of the model predictions of the 5 predicted plasma profiles with the experiments for JET Pulse No: 46664 t=6.0s (left) and 53521 at t=11.0s (right). Black solid curves correspond to the ITPA database value and red dashed and blue dash-dotted curve to predictions by the Bohm/GyroBohm and Weiland models, respectively.

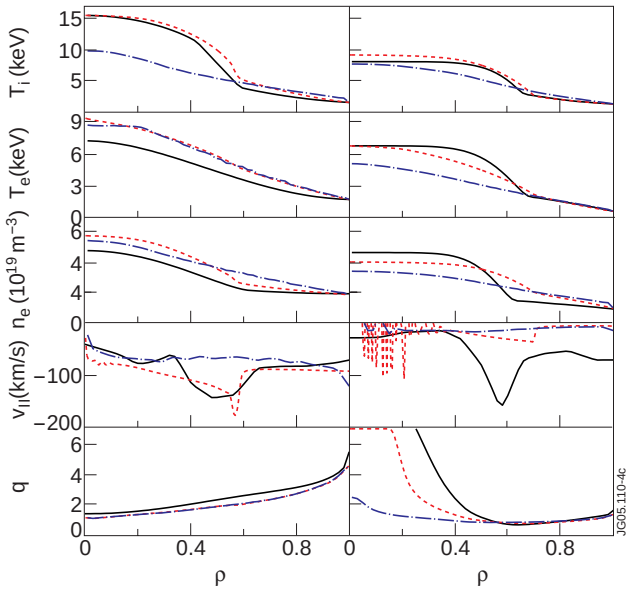

Figure 3: As in figure 2, but for JT-60U Pulse No: 34487 at t=5.0s (left) and 39056 at t=6.8s (right).

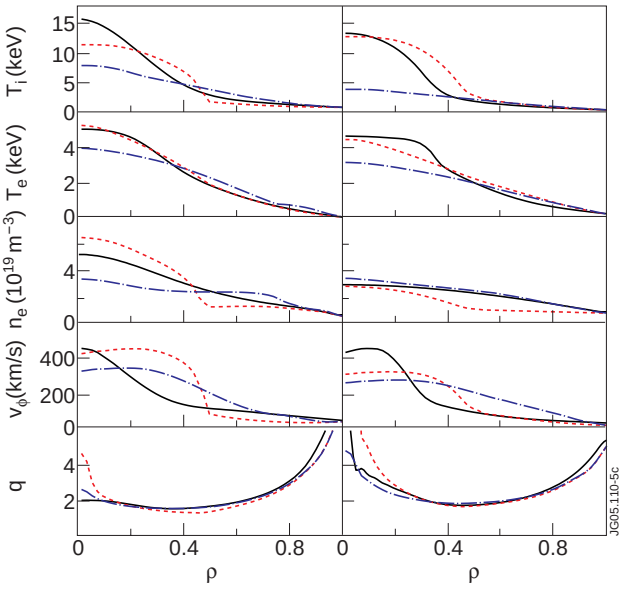

Figure 4: As in figure 2, but for DIII-D Pulse No: 87031 at t=1.85s (left) and 95989 at t=0.95s (right).

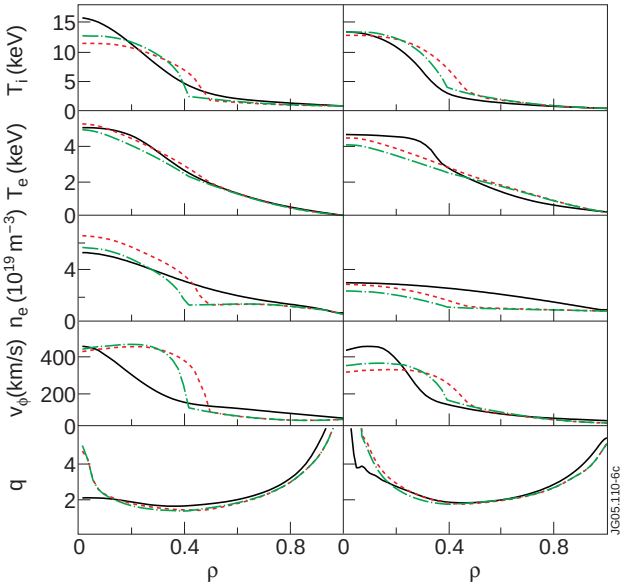

Figure 5: Effect of including the α-stabilisation in the Bohm/GyroBohm model for DIII-D Pulse No: 34487 at t=1.85s (left) and 39056 at t=0.95s (right). The black solid curves correspond to the experimental data and the red dashed (same curves an in figure 4) and green dash-dotted curves to the simulation predictions with taking into account the α-stabilisation and without it, respectively.

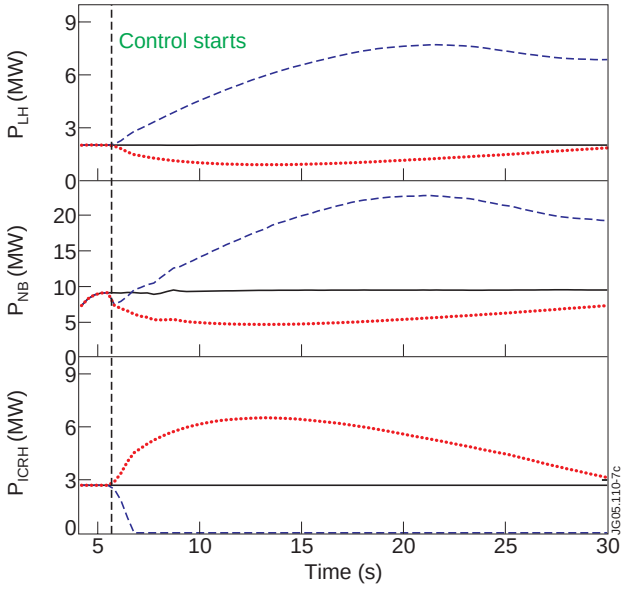

Figure 6: The power levels of LHCD, NBI and ICRH in two closed-loop (red and blue) and one open-loop (black) reference simulation.

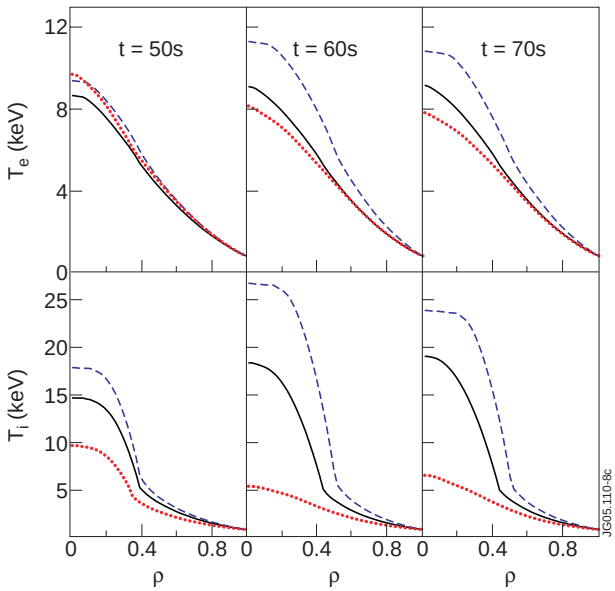

Figure 7: Electron and ion temperatures of the same three simulations with the same colour scheme as in figure 5. at three instants.

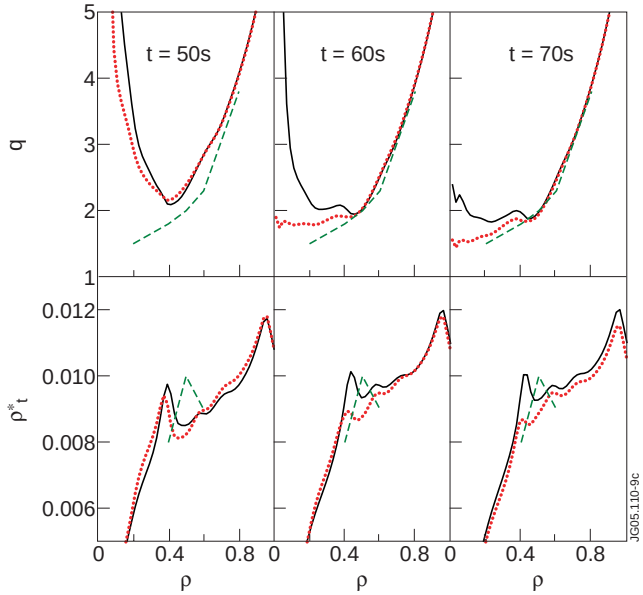

Figure 8: q and ρ_t^* for the closed-loop simulation (red) together with its set-point profiles (green dashed) and the open-loop reference simulation with constant power levels of the actuators (black).

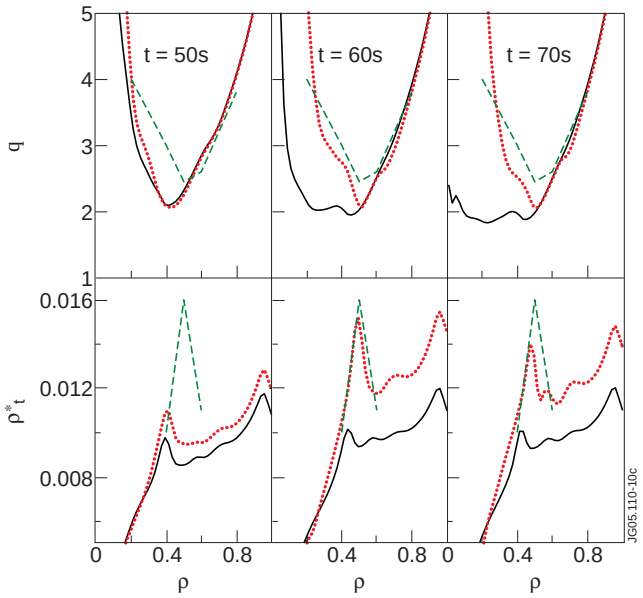

Figure 9: As in figure 7, but for the closed-loop simulation (blue) together with its set-point profiles (green dashed) and the open-loop reference simulations (black) (same as above).